Infrared Photodissociation Spectroscopy of Mg + (H 2 O)Ar n Complexes: Isomers in Progressive Microsolvation

ARTICLE *in* THE JOURNAL OF PHYSICAL CHEMISTRY A · SEPTEMBER 2005

Impact Factor: 2.69 · DOI: 10.1021/jp051877t · Source: PubMed

5 AUTHORS, INCLUDING:

Nicholas R Walker
Newcastle University
63 PUBLICATIONS **1,288** CITATIONS
SEE PROFILE

Ming-Kang Tsai
National Taiwan Normal University
22 PUBLICATIONS **539** CITATIONS
SEE PROFILE

Kenneth D Jordan
University of Pittsburgh
372 PUBLICATIONS **13,804** CITATIONS
SEE PROFILE

Infrared Photodissociation Spectroscopy of $Mg^+(H_2O)Ar_n$ Complexes: Isomers in Progressive Microsolvation

N. R. Walker,[†,‡] R. S. Walters,[†] M.-K. Tsai,[§] K. D. Jordan,[§] and M. A. Duncan*[,†]

Department of Chemistry, University of Georgia, Athens, Georgia 30602-2556 and Department of Chemistry, and Center for Molecular and Materials Simulations, University of Pittsburgh, Pittsburgh, Pennsylvania 15260

Received: April 11, 2005; In Final Form: June 15, 2005

Ion−molecule complexes of the form $Mg(H_2O)Ar_n^+$ ($n = 1-8$) are produced by laser vaporization in a pulsed-nozzle cluster source. These complexes are mass-selected and studied with infrared photodissociation spectroscopy in the O−H stretch region. The spectra are interpreted with the aid of ab initio calculations on the $n = 1-5$ complexes, including examination of various isomeric structures. The combined spectroscopic and theoretical studies reveal the presence of multiple isomeric structures at each cluster size, as the argon atoms assemble around the $Mg^+(H_2O)$ unit. Distinct infrared resonances are measured for argon-on-metal, argon-on-OH and argon-on-two-OH isomers.

Introduction

Ion−molecule complexes provide convenient model systems for studies of fundamental molecular interactions and the detailed potential energy surfaces that govern these. Spectroscopic studies have proven especially valuable for investigating the molecular structure of these complexes, including the role of isomeric species that may form.[1,2] Recently, metal-containing ions have been included in these studies.[3,4] Metal ion−water complexes are particularly interesting systems with which to explore the details of solvation.[5−22] Mass spectrometry studies,[5−9] ab initio calculations,[10−13] and various spectroscopic methods[14−22] have explored the structures and reactions of these systems. The competition between charge-dipole interactions and the growth of hydrogen bonding networks have been investigated in several recent studies.[20−22] In the present paper, we describe an infrared spectroscopic study of the $Mg^+(H_2O)$ complex in the OH stretch region as this system is progressively "solvated" by argon atoms. The potential around the cation−water system provides multiple binding sites for argon atoms, and the IR spectra reveal the isomeric structures that form.

Magnesium cation complexes with small molecules and rare gas atoms have been the subject of extensive studies in mass spectrometry,[5−9] electronic structure calculations,[10−13] and laser spectroscopy.[15−17] Collision-induced dissociation methods have determined various magnesium ion−ligand bond energies.[6] Magnesium cation−water clusters have been studied to investigate intracomplex reactions leading to charge separation ($Mg^+ \rightarrow Mg^{2+} + e^-$) and/or hydroxide formation.[7,8,11−13,16] These reactive processes appear to begin when the cation is solvated by five or more water molecules. Our research group has reported electronic spectroscopy of several Mg^+−L complexes near the strongly allowed 3s → 3p ($^2S \rightarrow {}^2P$) atomic transition of Mg^+ using ultraviolet laser photodissociation spectroscopy.[15,23] A detailed investigation of $Mg^+(H_2O)$ determined the structure of this ion and revealed information on its excited-state vibronic patterns.[15a] A similar study revealed the structure of the closely related $Ca^+(H_2O)$ ion.[15b] More recently, we have examined $Mg^+(CO_2)_n$ complexes with infrared photodissociation spectroscopy in the region of the CO_2 asymmetric stretch vibration.[24,25] These IR spectroscopy studies have been extended to $M^+(H_2O)$ complexes for M = V, Fe, Co, Ni.[21] In related infrared research, Inokuchi and co-workers studied the OH-stretch region of $Mg^+(H_2O)_{1-3}$ complexes, revealing the first appearance of hydrogen bonded water at $n = 3$.[22] The present IR spectroscopy builds on this latter work, examining the spectral changes that occur as argon atoms cluster around the $Mg^+(H_2O)$ system.

Rare gas or other weakly bound "spectator" adducts with ion−molecule complexes have been exploited by several research groups to enhance the measurement of photodissociation spectroscopy.[21,22,24−33] In the early experiments by Lee and co-workers, H_2 or N_2 were employed as the spectator,[26] but it is now more common to "tag" complexes with rare gas atoms such as neon or argon. As such tagging experiments developed, it became interesting to investigate the spectroscopic effects of the rare gas atoms on the spectroscopy.[30−32] Dopfer and co-workers have studied the attachment of multiple argon atoms on many small cation molecular complexes,[30] and Johnson and co-workers have investigated the influence of Ar atoms on the spectroscopy of many anion complexes.[31]

Our group has studied the infrared photodissociation spectroscopy of metal cation−molecular complexes with CO_2,[24] water,[21,25] acetylene,[25,33] and benzene.[33] In general, these complexes are more strongly bound than the molecular cations or anions that have been studied before, and rare gas tagging is essential for these studies. Our work on metal−cation water complexes includes studies of V^+, Co^+, Ni^+, and Fe^+ complexes[21] in addition to the present Mg^+ work. In the Fe^+−water system,[21b] we found evidence for isomeric structures in the attachment of one or two argon atoms and one or two water molecules. Inokuchi and co-workers found similar effects for the $Mg^+(H_2O)_{1-3}Ar$ complexes.[22] In the present study, we investigate $Mg^+(H_2O)Ar_n$ ($n = 1-8$) complexes with IR photodissociation spectroscopy and ab initio electronic structure calculations. This work began as an investigation of the Mg^+ interaction with water, but spectra for different argon adducts

* Corresponding author. E-mail: maduncan@uga.edu.
† University of Georgia.
‡ Present address: School of Chemistry, University of Bristol, Bristol BS8 1TS, U.K.
§ University of Pittsburgh.

10.1021/jp051877t CCC: $30.25
Published on Web 07/21/2005

eventually revealed additional interesting features of isomeric clusters based on argon binding sites.

Experimental Section

Clusters for these experiments are produced by laser vaporization in a pulsed supersonic expansion and mass analyzed in a reflectron time-of-flight mass-spectrometer (TOF-MS). The molecular beam apparatus, mass spectrometer, and laser methods used for infrared spectroscopy have been described previously.[25] The third harmonic of a Nd:YAG (355 nm) is used to vaporize a rotating magnesium rod, and water is added to the expansion gas via a few drops of liquid inserted into the gas flow at ambient conditions. Ionized $Mg^+(H_2O)Ar_n$ clusters are produced directly from the laser vaporization process in expansions of argon using a pulsed General Valve (1 mm nozzle) at 40 psi backing pressure and a 200 μs pulse duration. The free expansion is skimmed from the source chamber into the mass-spectrometer and the ions are extracted into the first drift region of the reflectron using pulsed acceleration voltages. Specific ions are mass-selected by pulsed deflection plates just before the reflectron field. Excitation and photodissociation occurs at the turning point in the reflectron field, where ions are overlapped with the output of the infrared laser. Parent and daughter ions are mass-analyzed in the second flight tube and mass spectra are recorded with a digital oscilloscope (LeCroy *WaveRunner* LT342). The data are transferred to a PC via an IEEE interface. Infrared resonance enhanced photodissociation (IR-REPD) spectra are obtained by monitoring the intensity of the fragment ions as a function of wavelength. All spectra are recorded in the mass channel corresponding to the loss of one argon atom from the selected parent ion.

The infrared laser is an optical parametric oscillator (OPO/OPA) system (Laser Vision) pumped by a Continuum 9010 Nd:YAG. This has two 532 nm-pumped KTP crystals in the grating tuned oscillator section and four KTA crystals in the amplifier section. The idler output from the oscillator is combined with residual 1064 nm in the amplifier, and difference frequency generation here provides the tunable near-IR output from 2.2 to 4.9 μm (4500−2050 cm^{-1}). In this experiment, the OPO is unfocused to prevent power broadening. Near 3500−3700 cm^{-1}, the laser pulse energies range from 8 to 10 mJ/pulse with an approximate line width of 0.3−0.5 cm^{-1}. Typical spectra are obtained at ∼1.0 cm^{-1} steps and averaged over 250 laser shots per step.

Computational Methodology

Ab initio electronic structure calculations using the Gaussian 03 program package[34] were carried out to aid in assigning the observed vibrational structure of the $Mg^+(H_2O)Ar_n$ ($n = 0-5$) clusters. For each cluster, the geometries were optimized at the MP2 level for various possible isomers differing in the locations of the Ar atoms. For each stationary point identified, the vibrational frequencies were calculated in the harmonic approximation, again using the MP2 method. For the $n = 0-3$ clusters, calculations were carried out treating all electrons explicitly and using the aug-cc-pVTZ basis set.[35a,b] For the $n = 0-2$ clusters calculations were also carried out using the aug-cc-pVQZ basis set[35b,c] to examine the suitability of the smaller aug-cc-pVTZ basis set, and CCSD(T)[36]/aug-cc-pVTZ calculations were carried out to explore the role of high-order correlation effects. Comparable all-electron calculations on the $n = 4-5$ clusters would be computationally prohibitive, and therefore, to examine these species, pseudopotentials[37,38] were adopted on the Mg and Ar atoms. The pseudopotentials were employed in conjunction with contracted 4s4p3d2f and 5s5p3d2f Gaussian-type basis sets for Mg and Ar, respectively, generated by augmenting the 2s2p Mg and 4s4p3d1f Ar basis sets of Stoll et al.[38] with diffuse functions. In the case of Mg, polarization functions were also taken from the corresponding aug-cc-pVTZ basis sets. As in the all-electron calculations, the aug-cc-pVTZ basis set was employed for the H and O atoms. To establish the magnitudes of the errors introduced by the adoption of the pseudopotentials, the $n = 0-3$ clusters were also characterized using pseudopotentials on the Mg and Ar atoms. In the discussion below, the calculations carried out using pseudopotentials are referred to as MP2/PP.

Several possible isomers were considered for the $n = 0-4$ clusters, whereas only a single structure was considered for the $n = 5$ cluster. In generating the initial structures, we were guided by the fact that the Ar atoms are expected to be able to bind to the H atoms as well as to the Mg^+ ion.

Results and Discussion

(a) Overview of Measured Spectra. As we have described previously, infrared photodissociation processes are inefficient in small ion−molecule complexes whose bond energies are significant compared to the infrared photon energies employed to excite vibrational fundamentals. In the $Mg^+(H_2O)$ complex, the cation−water bond energy is 28.4 kcal/mol (9940 cm^{-1}),[6c] and thus one-photon photodissociation is not possible in the 3500−3800 cm^{-1} region of the OH stretching vibration. The only possible exception to this occurs when there is incomplete cooling in the cluster growth process, as seen by Nishi and co-workers.[22] In this case, a small fraction of the complexes may have significant (about ≥6000 cm^{-1}) internal energy that adds together with the photon energy to achieve fragmentation. In such a case, the hot clusters have broad spectra. In our experiment, the cluster source is designed for more efficient cooling, and no IR photodissociation of the isolated $Mg^+(H_2O)$ complex is detected. To improve the photodissociation yield of $Mg^+(H_2O)$, Inokuchi and co-workers employed the rare gas tagging method,[22b] by making complexes containing a single argon atom. The binding energy for diatomic Mg^+Ar is 1295 cm^{-1}.[23b] Therefore, mixed $Mg^+(H_2O)Ar_n$ complexes can dissociate by elimination of argon following absorption in the OH stretch region of the spectrum.[22b] In the present work, we also use the argon tagging method with the $Mg^+(H_2O)$ complex, and we examine changes in the spectra that take place as multiple argon atoms are added to this system.

Figure 1 reports the IR photodissociation spectrum of the $Mg^+(H_2O)Ar$ complex under different experimental conditions. As shown in the upper trace, several bands are observed in the 3500−3800 cm^{-1} region, even though only two IR-active vibrations corresponding to the symmetric and asymmetric stretches of water are expected. We therefore anticipate the possible role of isomeric structures for these complexes. Indeed, Inokuchi and co-workers have reported two isomers, differing in the position of the single argon atom for the $Mg^+(H_2O)Ar$ complex.[22b] We therefore investigated the spectrum under different cluster source and dissociation laser conditions. In the upper trace of Figure 1, the cluster source was adjusted away from its optimum settings by increasing the vaporization laser power above its normal level and moving the its timing away from the most intense part of the pulsed gas expansion. These conditions produce clusters with incomplete cooling. The infrared laser was used at the highest laser pulse energy possible (∼20 mJ/pulse) in a "double-pass" configuration, producing a spectrum with rather broad vibrational resonances. In the center trace, the vaporization laser power and timing were adjusted to

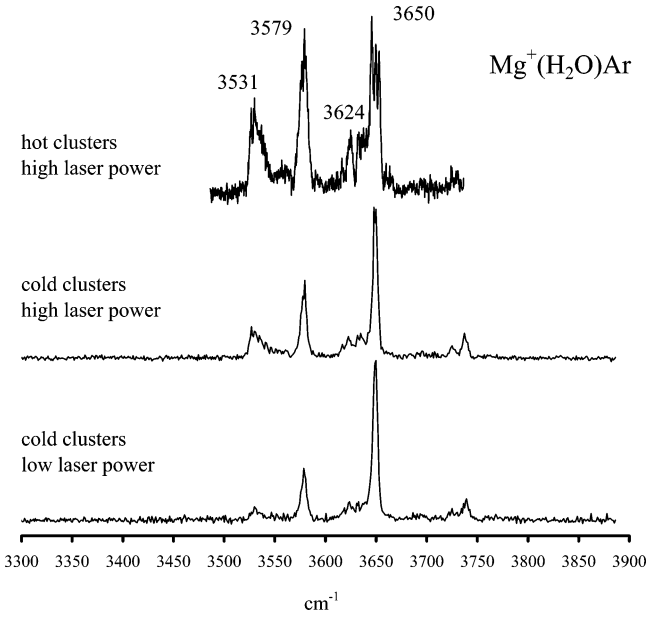

Figure 1. IR photodissociation spectrum of the $Mg^+(H_2O)Ar$ complex under different experimental conditions.

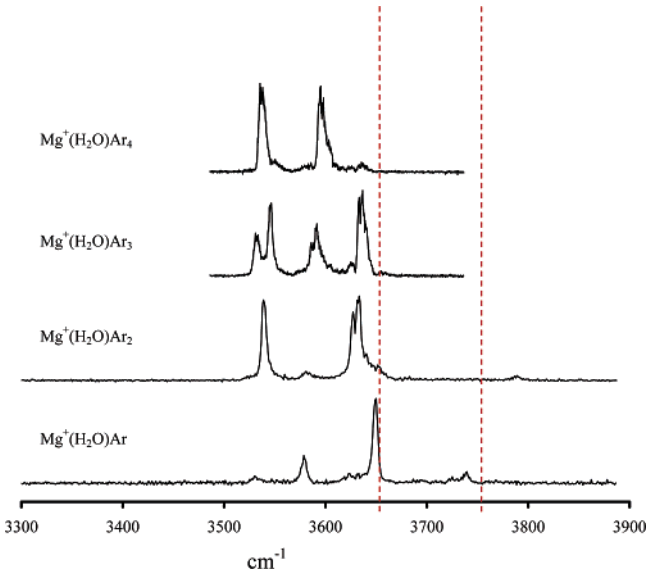

Figure 2. IR photodissociation spectrum of the $Mg^+(H_2O)Ar_n$, $n = 1-4$, complexes. The multiple peaks observed in each case suggest the presence of isomeric structures.

our normal settings known to produce colder clusters. The resulting spectrum contains essentially the same bands, but the lines are narrower and the intensity ratios have changed. Finally, the lower trace was obtained by reducing the laser pulse energy (~10 mJ/pulse) using only a single pass from the IR laser system. The bands are again relatively narrow, but the intensity ratios have changed again. In particular, the band near 3531 cm^{-1} has dropped to a level where it is almost missing. These patterns make sense if the bands at 3579/3650 and 3531/3624 cm^{-1} correspond to two different isomeric species, with the higher energy isomer being produced more effectively at higher temperature, and its weaker lines rising in relative importance at higher IR laser power because the more intense bands from the lower energy isomer are saturated.

These scans demonstrate that care must be taken with the conditions used to record spectra, particularly when different isomeric species are present. The relative intensities of different bands corresponding to different isomers can vary significantly depending on the experimental conditions. In principle, the relative isomer concentrations could be estimated via infrared *absorption* line intensities and calculated absorption strengths. However, we do not measure absorption spectra, but rather dissociation spectra, whose line intensities depend on both the absorption strength and the relative tendency for each isomer to dissociate. Therefore, we can detect the presence of different isomers but cannot be quantitative about their concentrations.

Figure 2 shows the spectra for the $Mg^+(H_2O)Ar_n$, $n = 1-4$, complexes obtained from measurements done under the cold conditions described above. The spectra of the $n = 1-3$ clusters contain multiple bands, again suggesting the presence of isomeric structures. All of the observed bands are shifted to the red of the symmetric (3657 cm^{-1}) and asymmetric (3756 cm^{-1}) stretch vibrations in the free water molecule (indicated by dashed vertical lines).[41] Such red shifts are expected because the metal cation withdraws bonding electron density from the highest molecular orbitals of water, and this reduces the stiffness of the OH bonds.[21] The cation−water binding is so strong that only the C_{2v} structure is expected for the $Mg^+(H_2O)$ subsystem of the complex. Thus the multiple bands seen here likely arise from isomers differing in the binding sites for the argon atoms. Binding of an Ar atom to Mg^+ should not significantly perturb the OH stretch vibrations, whereas binding of an Ar atom to an OH site should lead to an additional sizable red shift to the O−H stretching vibrations. These expectations are confirmed by detailed theoretical studies, as described below.

In principle, rotational band contours could be used to derive some structural information about these complexes. However, we find that the line widths measured here are independent of the laser line width in the range 0.3−1.0 cm^{-1}. This suggests that the complexes here are rotationally quite cold, and that the line widths are determined by the dynamics of the dissociation process rather than by rotational contours. We therefore focus on the comparison of vibrational bands with theory to determine the structures of these complexes.

(b) Calculated Structures and Energetics. To interpret these IR spectra, we investigate the structures and energetics of isomeric $Mg^+(H_2O)Ar_n$ complexes with various levels of ab initio calculations. The low-energy isomeric structures found for these complexes are presented in Figure 3. The Ar-atom binding energies and the OH stretch vibrational frequencies calculated for the various isomers are summarized in Tables 1 and 2. As seen from Figure 3, the Ar atoms can bind to the Mg^+ ion as well as to the OH groups. Surprisingly, the binding energies in these two sites are comparable, and this influences the relative energetics of all the structures investigated. In isomers with Ar atoms bound to the Mg^+ ion, the Ar atoms are found to be located along the side of Mg^+O axis. As we and others have discussed previously,[10,24] the binding of a water ligand, with the negative end of the dipole oriented toward the cation, induces a strong polarization of the 3s orbital, producing a lobe of negative charge in the region along the C_2 axis opposite the water monomer. Subsequent ligands, in this case Ar, avoid this negative charge region and instead bind along the side of the first ligand. This backside screening of the metal ion causes bent structures to form for Mg^+-L_2 complexes and trigonal pyramid structures to form for Mg^+-L_3 complexes.[10,24] It also limits the number of argon atoms that can bind to the Mg^+ ion.

The binding energies reported in Table 1 were obtained from MP2 calculations using

$$BE = E[Mg^+(H_2O)Ar_n] - E[Mg^+(H_2O)] - nE[Ar]$$

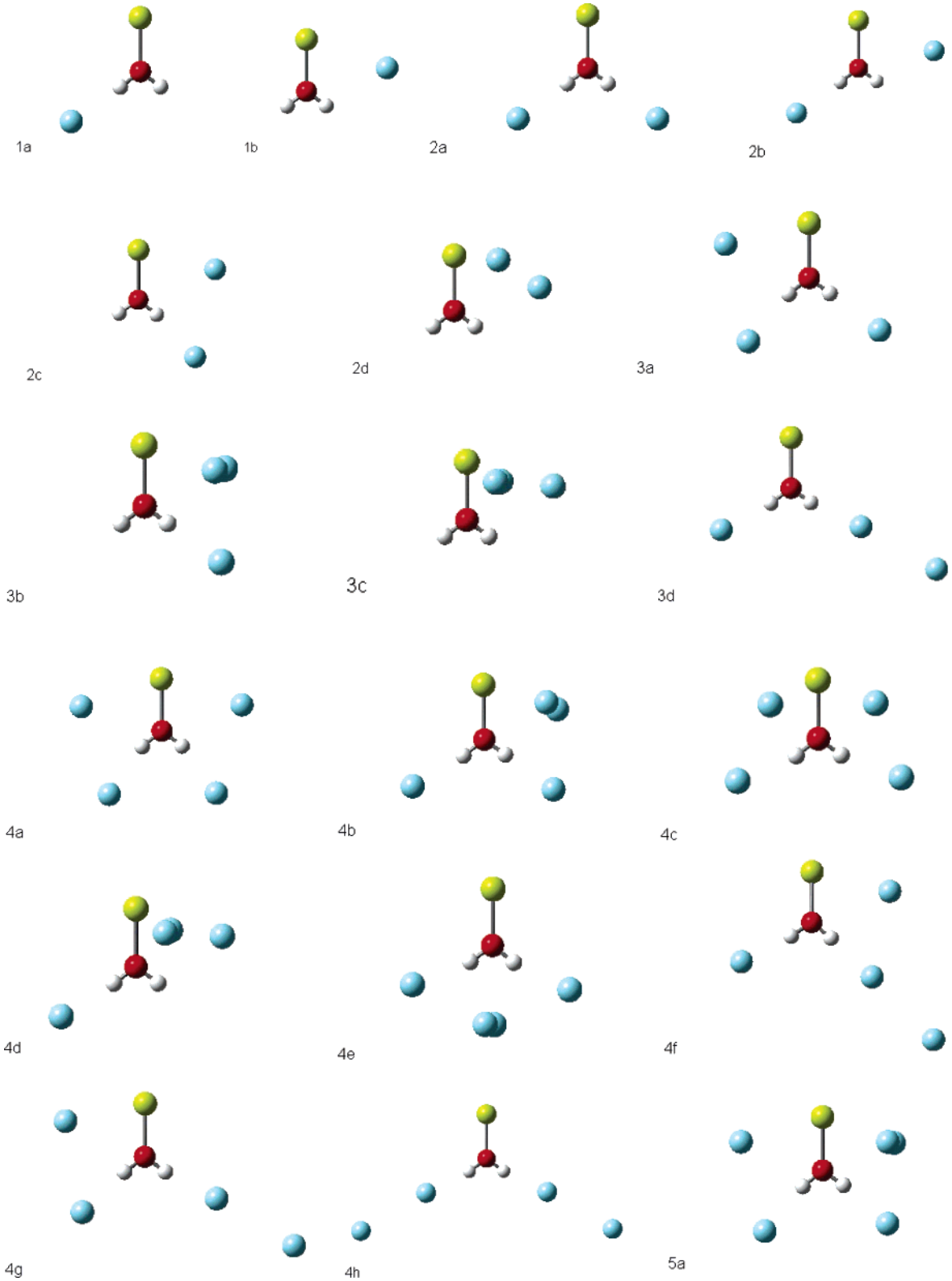

Figure 3. Geometries of the $Mg^+(H_2O)Ar_n$, $n = 1-5$, complexes, optimized using the MP2 procedure.

where the $Mg^+(H_2O)Ar_n$ energies include the counterpoise correction for basis set superposition error.[39,40] Table 2 reports the results of a more detailed study of the $Mg^+(H_2O)Ar_n$ ($n = 1-2$) complexes at different levels of theory, and Figure 4 reports the relative energies for the isomers at each cluster size.

In examining the trends in the calculated binding energies, we first consider results of the all-electron calculations on the $n = 1-3$ clusters. At the MP2/aug-cc-pVTZ level, two isomers, both with planar structures, were identified for $Mg^+(H_2O)Ar$. One isomer (1a) has the Ar atom bound to an H atom and the other (1b) has it bound in the vicinity of the Mg^+ ion. The ArMgO angle in 1b is calculated to be 73.3°. This strong deviation from a linear ArMgO arrangement is due to the polarization of the valence s orbital of the Mg^+ ion by H_2O, as discussed above. Even though 1b is referred to as Mg-bound, the Ar atom in this isomer also interacts strongly with one of

TABLE 1: Calculated Binding Energies (cm^{-1}), OH Stretch Frequencies (cm^{-1}), and Intensities of the $Mg^+(H_2O)Ar_n$, $n = 0-5$ Clusters[a]

			υ_s		υ_a	
isomers	BE w/o ZPE	BE with ZPE	freq	int[b]	freq	int[b]
H_2O			**3646**	**6**	**3766**	**75**
0			**3565**	**87**	**3653**	**223**
			3565	88	3653	227
1a	**770**	**587**	**3515**	**368**	**3635**	**278**
	792	603	3509	383	3631	276
1b	**682**	**561**	**3571**	**78**	**3662**	**236**
	n/a	n/a	n/a	n/a	n/a	n/a
2a	**1505**	**1169**	**3505**	**313**	**3578**	**648**
	1548	1215	3500	319	3571	661
2b	**1427**	**1163**	**3522**	**361**	**3639**	**315**
	n/a	n/a	n/a	n/a	n/a	n/a
2c	**1370**	**1105**	**3528**	**310**	**3639**	**266**
	1393	1130	3523	322	3635	267
2d	**1171**	**1013**	**3575**	**78**	**3667**	**227**
	1173	1017	3573	78	3664	232
3a	**2077**	**1677**	**3515**	**331**	**3588**	**559**
	2121	1726	3510	336	3583	577
3b	**1845**	**1530**	**3531**	**280**	**3644**	**281**
	1869	1554	3526	290	3641	283
3c	**1586**	**1396**	**3578**	**76**	**3670**	**218**
	n/a	n/a	n/a	n/a	n/a	n/a
3d	**1570**	**1209**	**3504**	**321**	**3576**	**683**
	1612	1256	3499	326	3570	696
4a	2594	2161	3526	310	3596	440
4b	2580	2135	3514	305	3589	606
4c	2468	2056	3515	267	3592	632
4d	2310	1969	3527	368	3645	285
4e	2221	1812	3509	220	3579	557
4f	2182	1765	3509	340	3580	604
4g	2183	1765	3509	354	3581	596
4h	1677	1297	3498	330	3568	729
5a	3025	2543	3525	298	3598	490

[a] Results obtained at the MP2 level of theory, with all binding energies being corrected for BSSE by means of the counterpoise procedure. The results indicated in bold are from the all-electron calculations using the aug-cc-pVTZ basis set. The remaining results are from pseudopotential calculations. The harmonic vibrational frequencies obtained from the all-electron and pseudopotential calculations have been scaled by 0.954. [b] Intensities are in units of km/mol (1 km/mol = 6.25×10^{28} cm/molecule). [c] 1b, 2b, and 3c isomers were found to be a local minimum in the all-electron but not found in the pseudopotential calculations.

the protons. The all-electron MP2/aug-cc-pVTZ calculations give Ar-atom binding energies of 770 and 682 cm^{-1} for 1a and 1b, respectively. Both expansion of the basis set from aug-cc-pVTZ to aug-cc-pVQZ and inclusion of high-order electron correlation effects act to preferentially stabilize 1b with respect to 1a, with the latter correction being more important. Vibrational zero-point energy (ZPE) corrections also stabilize 1b relative to 1a, and when the various corrections are combined, 1b is predicted to be slightly ($\sim$27 cm^{-1}) more stable than 1a.

The transition state for conversion of 1b to 1a is predicted to lie energetically less than 1 cm^{-1} above 1b at the MP2/aug-cc-pVTZ level. However, at the CCSD(T)//MP2/aug-cc-pVQZ level, the 1a $\rightarrow$ 1b and 1b $\rightarrow$ 1a barriers are calculated to be 60 and 28 cm^{-1}, respectively. Finally, with the inclusion of vibrational ZPE's calculated using MP2/aug-cc-pVQZ level harmonic frequencies, the barrier for isomerization of 1a to 1b is calculated to be 9 cm^{-1} and that for the reverse process is calculated to be 36 cm^{-1}. The harmonic frequencies of the bending mode corresponding most closely with motion along the isomerization pathway are calculated at MP2/aug-cc-pVQZ level to be 33 and 42 cm^{-1} for 1a and 1b, respectively. Actually, in constructing the adiabatic potentials for 1a/1b isomerization, the ZPE correction should exclude the isomerization coordinate. In that case the barriers for 1a $\rightarrow$ 1b and 1b $\rightarrow$ 1a isomerization are calculated to be 25 and 57 cm^{-1}, respectively, which leads us to conclude that it should be possible to observe both 1a and 1b experimentally.

Four isomers were characterized for the $Mg^+(H_2O)Ar_2$ complex. Three of these, 2a, 2b, and 2c, have planar structures. Isomer 2a has one Ar atom bound to each H atom. Isomers 2b and 2c have one Ar atom bound to an H atom and the other Ar atom bound near the Mg^+ ion in trans- and cis-like arrangements, respectively. Isomer 2d can be viewed as arising from an Ar dimer bound to the side of the $Mg^+(H_2O)$ complex. In this complex, one Ar atom lies close to the approximate Mg^+-(H_2O) plane and the other is located out-of-plane. 2a is calculated at the MP2/aug-cc-pVTZ level to be 78, 135, and 334 cm^{-1} more stable than 2b, 2c, and 2d, respectively. Attempts to locate a local minimum with the two Ar atoms bound on opposite sides of the Mg^+ ion failed at the MP2/aug-cc-pVTZ level; i.e., the optimization collapsed back to 2a. The net Ar-atom binding energies of 2a, 2b, 2c, and 2d, after allowing for basis set expansion, high-order correlation effects, and ZPE are calculated to be 1275, 1302, 1256, and 1201 cm^{-1}, respectively. The net Ar-atom binding energies in these clusters are approximately twice as large in magnitude as those for the single Ar atom of 1a and 1b.

Four isomers were identified for $Mg^+(H_2O)Ar_3$. At the MP2/aug-cc-pVTZ level the most stable of these 3a has an Ar atom bound to each H atom, and the third Ar atom bound near the Mg^+ ion. The three higher-energy isomers, 3b, 3c, and 3d, are calculated at the MP2/aug-cc-pVTZ level to be about 232, 491, and 507 cm^{-1} less stable than 3a, respectively. 3b has an Ar atom bound to one of the H atoms and an Ar dimer bound near the Mg^+ atom, with one of the Ar atoms of the dimer located above and the other below the $Mg^+(H_2O)$ plane. 3c can be viewed as being derived from an Ar trimer bound to the side of the $Mg^+(H_2O)$ complex with the two Ar atoms closest to Mg^+ being located above and below the plane of the $Mg^+(H_2O)$ species. The high-energy isomer 3d has an Ar atom bound to one H atom and an argon dimer bound the other H atom in an approximately linear arrangement. Attempts to optimize a planar $Mg^+(H_2O)Ar_3$ isomer with one Ar atom bound to an H atom and the remaining two Ar atoms bound to the Mg^+ ion on opposite sides of the MgO bond proved unsuccessful as such structures were unstable with respect to collapse back to 3a.

The pseudopotential calculations give Ar-atom binding energies and vibrational frequencies for the $Mg^+(H_2O)Ar_n$, $n = 1-3$, clusters very close to the corresponding all-electron results. One difference is that the pseudopotential calculations fail to give minima for isomers 1b and 2b. This is not surprising because the all-electron MP2/aug-cc-pVTZ calculations gave a barrier of less than 1 cm^{-1} for conversion of 1b to 1a. The barrier for isomerization of 2b $\rightarrow$ 2a is not calculated at the MP2/aug-cc-pVTZ level but is probably very low. It is anticipated that with the use of a more flexible basis set and inclusion of high-order correlation effects, the pseudopotential calculations could locate the 1b and 2b minima.

Eight isomers were identified for $Mg^+(H_2O)Ar_4$. All of these, with the exception of 4d, have Ar atoms bound to each H atom. The three most stable isomers, 4a, 4b, and 4c, all have one Ar atom bound to each H atom. In the most stable of these, 4a, the remaining Ar atoms are bound to Mg^+ on either side of the Mg^+O bond. The second most stable isomer of $Mg^+(H_2O)Ar_4$, 4b, has the other two Ar atoms bound as a dimer to the Mg^+ ion with one Ar above and one Ar below the $Mg^+(H_2O)$ plane.

TABLE 2: Ar Atom Binding Energies (cm^{-1})[a] and Relative Zero-Point Energies (cm^{-1}) for $Mg^+(H_2O)Ar_n$, $n = 1-2$, at Different Levels of Theory

isomer	MP2/TZ[b]	MP2/QZ[c]	CCSD(T)/TZ//MP2/TZ[d]	CCSD(T)/QZ//MP2/QZ[d]	ΔZPE/TZ[e]	ΔZPE/QZ[e]	total/TZ[f]	total/QZ[f]
1a	770	813	772	810	183	175	589	634
TS	682	728	713	750	115	125	599	625
1b	682	737	723	778	121	117	602	661
2a	1505	1587	1512	1583	336	309	1175	1275
2b[g]	1427	1515	1466	1554[h]	264	252	1202	1302[h]
2c	1370	1465	1421	1512	265	256	1156	1256
2d	1171	1272	1258	1359[h]	157	158	1100	1201[h]

[a] All binding energies include the counterpoise correction for BSSE. [b] From MP2/aug-cc-pVTZ optimizations [c] From MP2/aug-cc-pVQZ optimizations. [d] The CCSD(T) calculations were carried out at MP2/aug-cc-pVTZ or aug-cc-pVQZ optimized geometries. [e] $\Delta ZPE = ZPE[Mg^+(H_2O)Ar] - ZPE[Mg^+(H_2O)]$ at MP2/aug-cc-pVTZ or MP2/aug-cc-pVQZ. [f] $E(\text{total/TZ}) = E(\text{CCSD(T)/TZ//MP2/TZ}) + E(\Delta ZPE/TZ)$, and $E(\text{total/QZ}) = E(\text{CCSD(T)/QZ//MP2/QZ}) + E(\Delta ZPE/QZ)$. [g] This nonminimum structure has one Ar atom bound near Mg^+ ion and the other bound to a H atom in a trans-like arrangement. [h] Estimated values. $E(\text{CCSD(T)/QZ//MP2/QZ})$ is estimated by $E(\text{MP2/QZ}) + E(\text{CCSD(T)/TZ//MP2/TZ}) - E(\text{MP2/TZ})$.

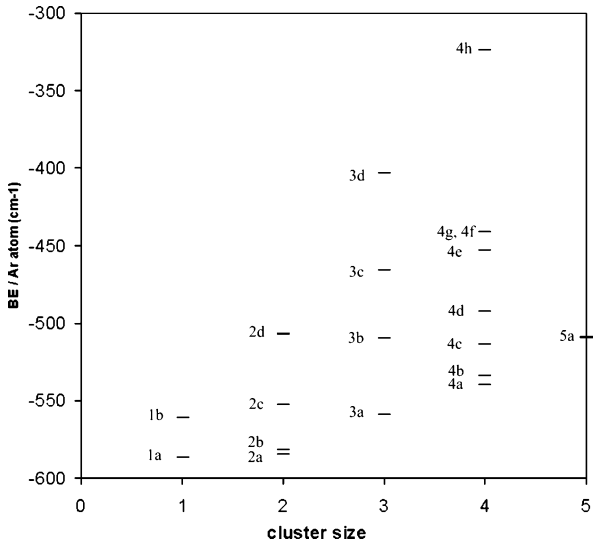

Figure 4. Average Ar atom binding energies per Ar atom for the $Mg^+(H_2O)Ar_n$ isomers calculated MP2 theory level. These results for the $n = 1-3$ clusters are from all-electron MP2/aug-cc-pVTZ calculations and those for the large clusters are from MP2/PP calculations. Corrections for BSSE and for vibrational ZPE's have been applied. The latter corrections come from the MP2-level harmonic frequencies scaled as described in the text.

Isomer 4c has an Ar dimer bound above the plane of the $Mg^+(H_2O)$ in the vicinity of the Mg^+. 4d has an Ar trimer bound along the Mg^+O axis, with the fourth Ar atom bound on the remote H atom. Isomer 4e has one Ar atom bound to each H atom and an Ar dimer bound between two OH groups and perpendicular to the plane of $Mg^+(H_2O)$. The sixth and seventh isomers of $Mg^+(H_2O)Ar_4$ lie appreciably higher in energy and have an Ar atom bound to one H atom, an Ar dimer bound to the other H atom, and a single Ar atom bound to Mg^+. The least stable isomer identified for $Mg^+(H_2O)Ar_4$, 4h, has an Ar dimer bound to each H atom. The only isomer characterized for $Mg^+(H_2O)Ar_5$ has an Ar atom bound to each H atom, and three Ar atoms bound near the Mg^+ ion, with two of these located out of the $Mg^+(H_2O)$ plane.

(c) Calculated Vibrational Spectra. To facilitate comparison between theory and experiment, the calculated OH stretch vibrational frequencies have been scaled by a factor of 0.954, chosen so as to bring the calculated harmonic frequencies at MP2/aug-cc-pVTZ of the OH stretch modes of the free water monomer into close agreement with its well-known experimental frequencies. The scaled frequencies are summarized in Table 1. In the ensuing discussion, these scaled frequencies are employed.

The OH stretch frequencies of the $Mg^+(H_2O)$ complex are calculated to be 3565 (symmetric stretch) and 3653 cm^{-1} (asymmetric stretch), which are shifted to the red by 92 and 103 cm^{-1}, respectively from the measured frequencies of the OH stretch vibrations of the isolated water molecule.[41] As for the isolated water molecule, the asymmetric OH stretch vibration has the higher frequency. These red shifts are due to charge transfer from the water toward the metal, as we have discussed previously.[21] Unfortunately, the infrared spectrum for the untagged $Mg^+(H_2O)$ complex has not been measured, so comparison of theory with experiment is not possible for this species.

For isomer 1a of $Mg^+(H_2O)Ar$, the calculations predict the symmetric and asymmetric OH stretch vibrations to have additional red shifts of 50 and 18 cm^{-1}, respectively, compared to the corresponding vibrations of $Mg^+(H_2O)$. The interaction with the Ar atom causes some localization of the vibrations, making the use of the "symmetric" and "asymmetric" labels only approximate. The more red-shifted transition is that associated with the OH stretch vibration more localized on the OH to which the Ar atom is attached. The binding of the Ar atom to OH causes a small increase in the length of the associated OH bond (calculated increase of 0.0036 Å), and this in turn is accompanied by a red shift of the associated OH stretch vibration. In contrast, for isomer 1b of $Mg^+(H_2O)Ar$, in which the Ar atom is located near the Mg^+ ion, the calculated frequencies of the OH stretch vibrations are weakly ($6-9$ cm^{-1}) *blue* shifted relative to the corresponding frequencies of $Mg^+(H_2O)$. The inductive effect that causes a red shift in the OH stretch vibrations of $Mg^+(H_2O)$ relative to those of a free water molecule is partially mediated when an Ar atom is bound to the metal ion, thus slightly reducing the red shifts.

The symmetric and asymmetric OH stretch frequencies of isomer 2a of $Mg^+(H_2O)Ar_2$, with Ar atoms bound to each H atom, are predicted to be red shifted by 60 and 75 cm^{-1}, respectively, compared to the corresponding vibrations of $Mg^+(H_2O)$. The calculated frequencies of OH stretch vibrations of the "trans" and "cis" isomers 2b and 2c are less red shifted than those of 2a and are, in fact, close to those of 1a, which has only one Ar atom bound to OH. The symmetric and asymmetric OH stretch frequencies of isomer 2d, with two Ar atoms bound to Mg^+ ion, are predicted to be blue shifted relative to the corresponding vibrations of $Mg^+(H_2O)$ by 10 and 14 cm^{-1}, respectively.

The calculated OH stretch frequencies of isomer 3a of $Mg^+(H_2O)Ar_3$ are close to those of 2a, again consistent with the observation that an Ar atom bound near the Mg^+ ion has little effect on frequencies of the OH stretch vibrations. Similarly, the calculated frequencies of the OH stretch vibrations of 3b

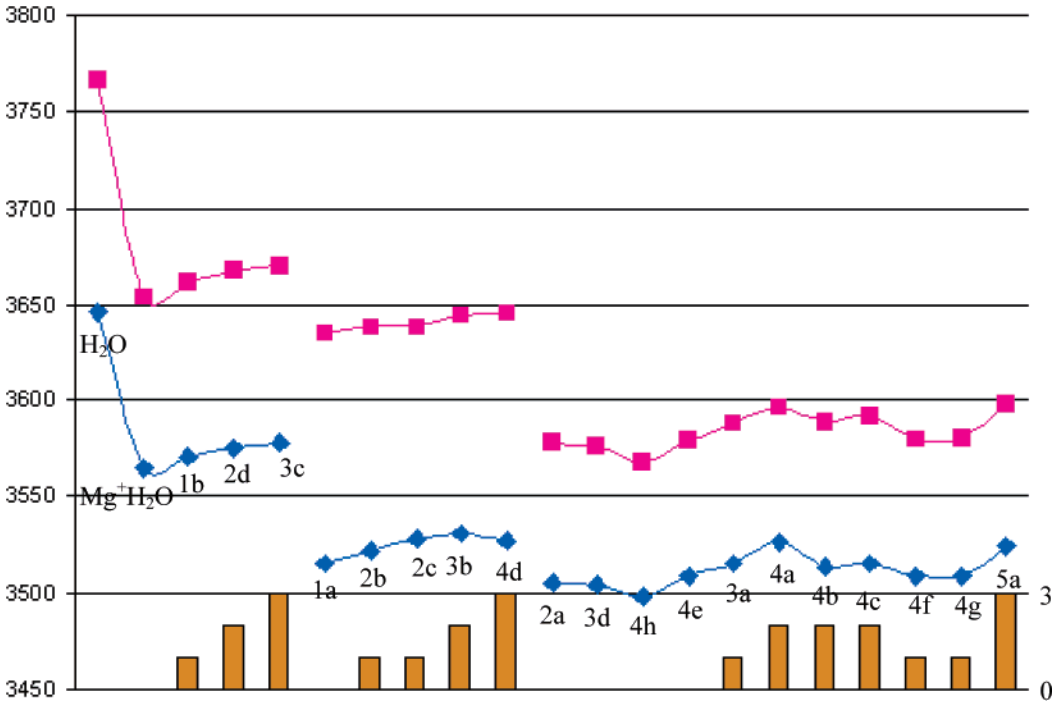

Figure 5. Summary of the calculated OH stretch frequencies of the $Mg^+(H_2O)Ar_n$ clusters. The left axis denotes the calculated OH stretch frequencies (cm^{-1}) for the asymmetric stretch (pink) and symmetric stretch (blue) for each complex. The histograms at the bottom are referenced to the right axis to denote the number of Ar atoms bound to Mg^+ ion in each complex.

are close to those of 2c, and the calculated frequencies of 3c are close to those of 2d. Finally, isomer 3d has OH stretch frequencies nearly identical to those of 2a, demonstrating that the binding of an Ar dimer to one of the OH groups (as in 3d) has nearly the same impact on the OH stretch frequencies as the binding of a single Ar atom.

The above discussion of the influence of the Ar atoms on the frequencies of the OH stretch vibrations of $Mg^+(H_2O)Ar_n$, $n = 1-3$, clusters was based on the results of the all-electron calculations. For these species nearly the same vibrational frequencies are obtained from the pseudopotential as from the all-electron calculations. Thus we can confidently adopt the pseudopotential procedure for discussing the trends in the vibrational frequencies for the larger clusters.

The calculated OH stretch frequencies of the 4a isomer of $Mg^+(H_2O)Ar_4$ with an Ar atom bound to each OH group and two Ar atoms bound to the Mg^+ ion fall slightly to the blue to those calculated for 3a, whereas the calculated frequencies of 4b and 4c are essentially identical to those of 3a. Isomers 4e, 4f, and 4g are all predicted to have similar OH stretch vibrations, red shifted by about 17 cm^{-1} with respect to those of 4a, whereas 4h, with an Ar dimer bound to each H atom, has the most red shifted OH stretch vibrations of the various $Mg^+(H_2O)Ar_4$ isomers. However, the last four isomers of $Mg^+(H_2O)Ar_4$ are calculated to be about 400 cm^{-1} less stable than 4a and are unlikely to be very important under the conditions of the experiments.

The only isomer characterized for $Mg^+(H_2O)Ar_5$, 5a, has three Ar atoms bound in the vicinity of the Mg^+ ion, and one Ar atom bound to each OH. 5a is calculated to have nearly the same OH stretch vibrational frequencies as 4a which also has one Ar atom bound to each H atom. The extra Ar atom bound to Mg^+ in 5a has only a minor effect on the OH stretch frequencies. The calculated OH stretch frequencies are summarized in Figure 5, from which the large red shifts associated

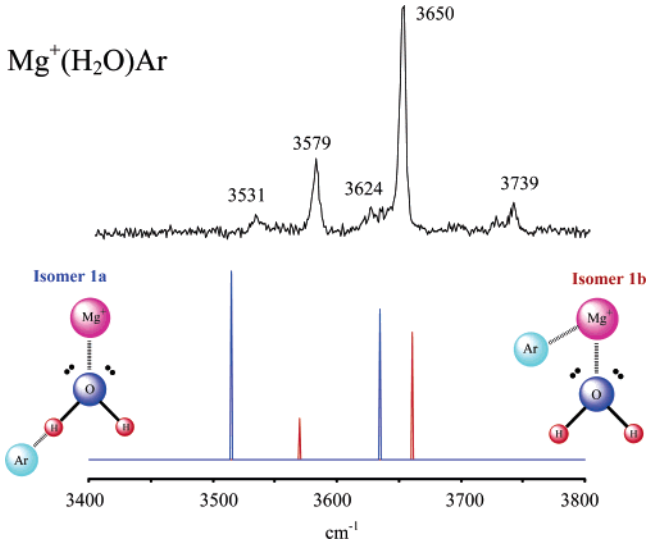

Figure 6. Comparison of calculated and measured vibrational spectra of the $Mg^+(H_2O)Ar$. The calculated spectrum of isomer 1a is shown in blue, and that for 1b is shown in red.

with binding of Ar atoms on H atoms and the small blue shifts resulting from the binding of Ar atoms near Mg^+ are readily apparent.

(d) Comparison between Calculated and Measured Vibrational Spectra. *i. $Mg^+(H_2O)Ar$.* Figure 6 compares the measured vibrational spectrum of $Mg^+(H_2O)Ar$ to the calculated spectra for the 1a and 1b isomers. The experimental spectrum has strong vibrational transitions at 3579 and 3650 cm^{-1}, with weaker transitions at 3531, 3624, and 3739 cm^{-1}. Weak bands in the 3700−3800 cm^{-1} region are present in the vibrational spectra of many $M^+(H_2O)Ar_n$ complexes and are due to combination bands involving Ar vibrations.[21] Thus we conclude that the 3739 cm^{-1} feature in the spectrum of $Mg^+(H_2O)Ar$ is a combination band involving OH stretch and either Ar−H or Ar−Mg^+ stretch. In this work, we are primarily interested in

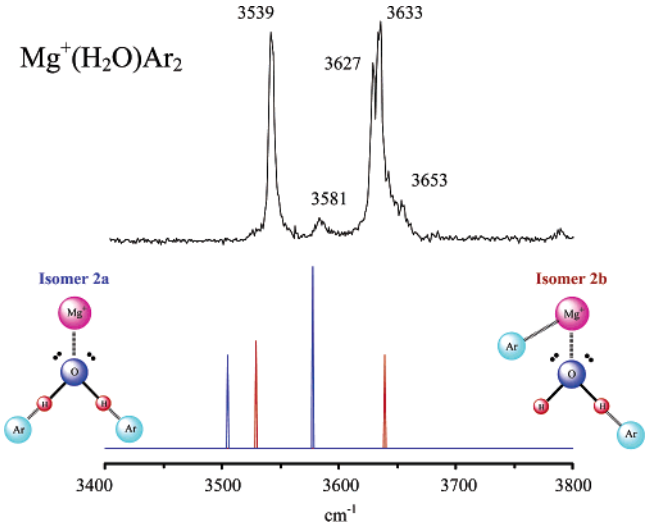

Figure 7. Comparison of calculated and measured vibrational spectra of the $Mg^+(H_2O)Ar_2$. The calculated spectrum of isomer 2a is shown in blue, and that for 2b is shown in red.

the assignments of the OH stretching fundamentals and will not further consider weak structure due to combination bands.

The relative intensities of the observed strong and weak transitions of $Mg^+(H_2O)Ar$ depends on the experimental conditions, as shown in Figure 1, indicating the presence of two isomers. The spectrum shown in Figure 6 is the one measured under our coldest conditions, which is assumed to favor the most stable isomer. The calculated OH stretch frequencies of isomer 1a (indicated by blue peaks) correspond closely to the positions of the two weak peaks in the experimental spectrum, and the calculated OH stretch frequencies of isomer 1b (indicated in red) to the two intense peaks. Although 1a is calculated to be 88 cm^{-1} more stable than 1b at the MP2/aug-cc-pVTZ level of theory, expansion of the basis set (from aug-cc-pVTZ to aug-cc-pVQZ), inclusion of high-order correlation effects (at the CCSD(T) level), and correction for vibrational zero-point energy (calculated at the MP2/aug-cc-pVQZ level) act to stabilize 1b relative to 1a. As noted above, combination of all these corrections leads to the conclusion that 1b is about 27 cm^{-1} more stable than 1a. This conclusion is consistent with the experiment, as the two strongest peaks in the spectrum match well the predicted bands for 1b in both position and relative intensity.

ii. $Mg^+(H_2O)Ar_2$. The experimental and calculated spectra of $Mg^+(H_2O)Ar_2$ are compared in Figure 7. The measured spectrum has an intense peak at 3539 cm^{-1}, an intense "doublet" at 3627 and 3633 cm^{-1}, and weak features at 3581 and 3653 cm^{-1}. The intense bands fall very close to the frequencies predicted for isomers 2b and 2c (although, only a single line is predicted in the vicinity of the intense doublet). The doublet observed near 3630 cm^{-1}, may indicate that both of these cis and trans isomers are contributing to the experimental spectrum.

The weak band observed at 3581 cm^{-1} is close to the position predicted for the higher frequency vibration of the 2a isomer, but there is no peak in the experimental spectrum corresponding to the lower frequency OH stretch vibration of 2a, which is calculated to occur at 3505 cm^{-1}. We also have an unassociated shoulder at 3653 cm^{-1}. This feature plus and the 3581 cm^{-1} band could conceivably derive from an isomer with Ar atoms bound to Mg^+ on either side of the MgO axis. Although such a species was not found to be a minimum at the MP2 level, such a species could be a local minimum at the CCSD(T) level, particularly after inclusion of vibrational ZPE corrections.

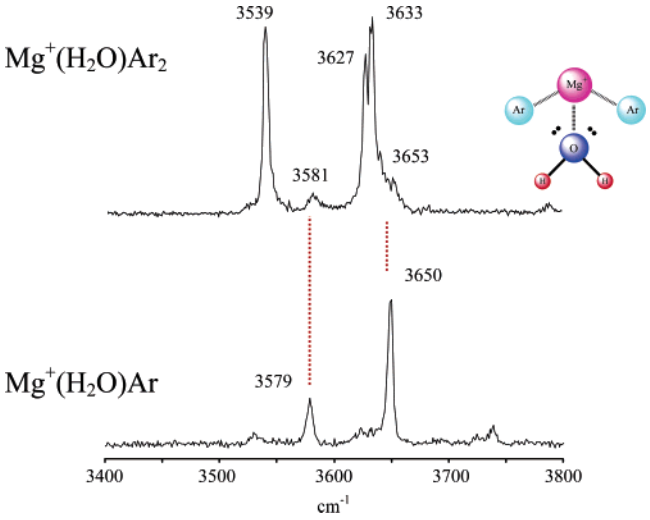

Figure 8. Comparison of the spectrum measured for $Mg^+(H_2O)Ar_2$ to that for $Mg^+(H_2O)Ar$, whose major bands arise from isomer 1b. The weak bands at 3581 and 3653 cm^{-1} match almost perfectly with the bands for the 1b isomer, providing evidence for a minor population of an isomer with both argons bound to Mg^+.

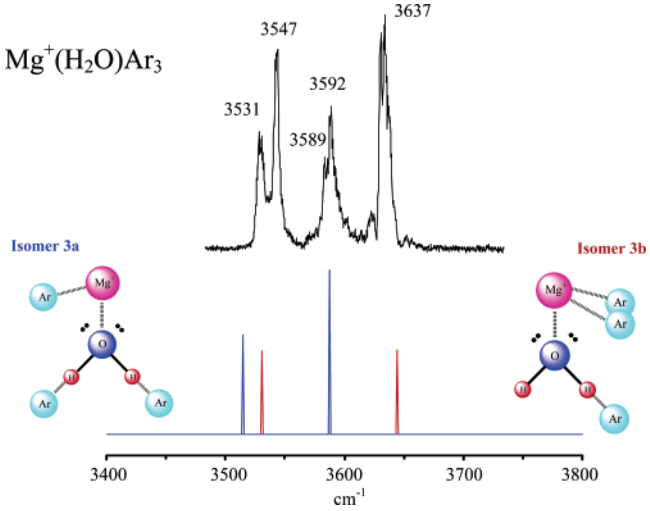

Figure 9. Comparison of the experimental spectrum for the $Mg^+(H_2O)Ar_3$ complex with the predictions of theory. The calculated spectrum of isomer 3a is shown in blue, and that for 3b is shown in red.

Because there are no argons bound to an OH, such an isomer would be expected to have OH stretch frequencies close to those of 1b. As shown in Figure 8, the spectrum of the 1b isomer matches almost exactly with the weak bands observed near 3581 and 3653 cm^{-1}. Therefore, it appears that we do have a small amount of this "two-argons-on-Mg^+" isomer, and little or no concentration of isomer 2a.

iii. $Mg^+(H_2O)Ar_3$. Figure 9 compares the experimental and calculated spectra of $Mg^+(H_2O)Ar_3$. The experimental spectrum has intense peaks at 3531, 3547, 3592, and 3637 cm^{-1}. The frequencies of the two more intense peaks are close to those calculated for isomer 3b, and the frequencies of the two less intense peaks correspond closely to those calculated for isomer 3a. Although the MP2/aug-cc-pVTZ calculations predict isomer 3a to be about 232 cm^{-1} more stable than 3b, upon inclusion of vibrational ZPE, the energy difference is calculated to be only 147 cm^{-1}. On the basis of results for $Mg^+(H_2O)Ar$ and $Mg^+(H_2O)Ar_2$, it is anticipated that calculations using the more flexible aug-cc-pVQZ basis set and including high-order correlation effects would predict 3b to be slightly more stable than 3a, consistent with slightly more intense peaks associated with

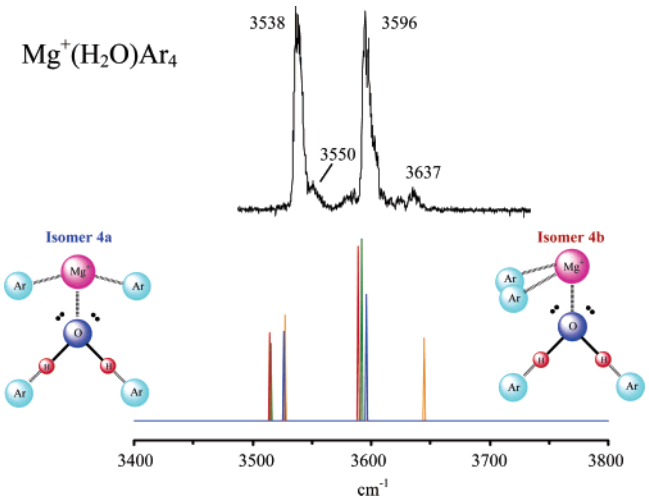

Figure 10. Comparison of the experimental spectrum for the $Mg^+(H_2O)Ar_4$ complex with the predictions of theory. The calculated spectrum of isomer 4a is shown in blue, and that for 4b is shown in red. Predicted spectra for 4c and 4d are shown in green and orange, respectively.

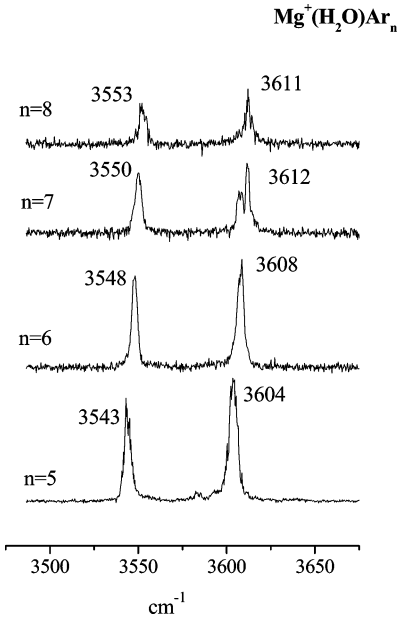

Figure 11. Spectra for the $Mg^+(H_2O)Ar_n$ complexes for $n = 5-8$.

3b than 3a in the observed spectrum. Isomers 3c and 3d are calculated to be 281 and 465 cm^{-1} less stable, respectively, than 3a at the MP2/aug-cc-pVTZ level with ZPE corrections, and it is unlikely that either of these has appreciable population under the experimental conditions.

iv. $Mg^+(H_2O)Ar_4$. Figure 10 compares the calculated and experimental vibrational spectra of $Mg^+(H_2O)Ar_4$. The experimental spectrum displays intense peaks near 3538 and 3596 cm^{-1}, together with weak features near 3550 and 3637 cm^{-1}. The frequencies associated with the two observed intense peaks are close to those calculated for the OH stretch vibrations of isomers 4a and 4b, with the calculated frequencies being 3526 and 3596 cm^{-1} for 4a and 3514 and 3589 cm^{-1} for 4b. The frequency differences between 4a and 4b are great enough that if both were highly populated, the experimental spectra should display two pairs of intense doublets. Because doublets are not observed, we conclude that only one of these isomers is present in high population in the experiment. The MP2/pseudopotential calculations with the inclusion of ZPE corrections predict 4a to be 26 cm^{-1} more stable than 4b. However, the relative stability of the two isomers could be reversed upon adoption of a more flexible basis set and inclusion of high-order correlation effects. Support for this possibility is provided by the experimental spectrum because each intense line is accompanied by a weak shoulder to the blue. Thus we favor the interpretation that the two intense lines are due to 4b, with the weak shoulders to the blue being due to 4a. The OH stretch frequencies calculated for isomer 4c are very close to those of isomer 4b, and it is possible that this isomer is also present experimentally. The calculated OH stretch frequencies of 4d match well with the weak bands observed at 3550 and 3637 cm^{-1}. The higher frequency OH stretch bands of 4e, 4f, and 4g isomers are calculated to fall between 3579 and 3581 cm^{-1}, close to the shoulder of weak intensity near 3580 cm^{-1}. However, the lower frequency OH stretch band of each of these isomers is predicted to fall at 3509 cm^{-1} and there is no evidence of a low energy shoulder on the observed intense line at 3538 cm^{-1}. The fact that the 3550 and 3637 bands fall very close to the positions of the bands seen for the 3b isomer of $Mg^+(H_2O)Ar_3$, supports the interpretation that 4d is present at low population.

Theory and experiment agree that there are basically three isomer types for the $n \leq 4$ $Mg^+(H_2O)Ar_n$ clusters. Isomers with no Ar atoms bound to OH are observed for the $n = 1$ and 2 clusters. These species have OH frequencies that are red shifted from those in the isolated water molecule due to the effect of the metal ion withdrawing bonding electron density from the water molecule. Isomers that have one argon atom bound to OH are observed for each of the $n = 1-4$ clusters. These are of minor importance for the $n = 1$ and 4 clusters and of major importance in the $n = 2$ and 3 clusters. The red shifts of the OH stretch vibrations of these isomers are greater than for those isomers with no Ar atoms bound to OH. The third type of isomer has Ar atoms bound to each OH group. These isomers experience significant additional red shifts compared to those species with only one Ar atom on OH. This type of isomer is apparently present only as a minority species for the $n = 2$ cluster. However, for the $n = 3$ cluster this type of isomer (3a) with Ar atoms bound to each OH group has roughly the same population as the isomer with only one Ar on OH (3b), and in the $n \geq 4$ clusters, isomers with Ar atoms bound to both OH groups dominate. The binding of additional argon atoms on the metal ion has a relatively minor effect on the OH frequencies, regardless of the exact position.

It is encouraging that the electronic structure calculations identify the major isomers detected in the experiments and successfully account for the dominant peaks in the measured vibrational spectra. However, as the more extensive calculations on the smaller clusters illustrate, it is a significant challenge to establish the correct energy orderings of the isomers. Not only are very large basis sets and inclusion of high-order correlation effects (e.g., at the CCSD(T) level) required, but also vibrational ZPE corrections are important. Given the weak binding of the Ar atoms to the $Mg^+(H_2O)$ core, the ZPE energies should clearly be calculated by allowing for vibrational anharmonicity, a daunting task when ab initio energies are used.

(e) Larger Clusters. Figure 11 shows the IR spectra measured for the larger $Mg^+(H_2O)Ar_n$ clusters ($n = 5-8$). All of these spectra consist of only two vibrational bands (although the higher frequency band is split into a doublet in the $n = 7$ cluster) which shift to the blue with increasing number of Ar atoms. At $n = 5$, the two bands occur at 3543 and 3604 cm^{-1}, slightly to the blue of the positions of the corresponding bands in the spectra of the $n = 4$ complex at 3538 and 3596 cm^{-1}. The only isomer of $Mg^+(H_2O)Ar_5$ investigated theoretically, 5a,

has vibrational bands predicted at 3525 and 3598 cm^{-1}, very close to the observed bands. 5a has three Ar atoms bound to the metal ion and one bound to each OH site of the water molecule.

The similarity of the spectra for the $n \geq 4$ clusters implies that all of these species have at least one Ar atom bound to each OH group, with the remaining Ar atoms bound in the vicinity of the Mg^+ ion. The blue shifts in going from $n = 6$ to 7 and from 7 to 8 are smaller than those between $n = 4$ and 5 and between 5 and 6. This suggests that all Ar atoms in the vicinity of the Mg^+ ion are directly bound to the ion in the $n = 4$, 5, and 6 clusters, but that the additional Ar atoms in the $n = 7$ and 8 clusters are bound in a second solvent shell as would occur if they were bound as Ar_3 trimers as in 3c and 4d. Johnson and co-workers have reported the observation of an icosahedral shell closing when 12 argon atoms enclose the $Cl^-(H_2O)$ core ion.[31g] However, we were not able to produce sufficient population of clusters in the size range near $n = 12$ to obtain their spectra.

Conclusions

$Mg^+(H_2O)Ar_n$ complexes have been studied in detail with infrared photodissociation spectroscopy and ab initio electronic structure calculations. Both the vibrational predissociation spectra and the calculations indicate that there are multiple isomers differing in the attachment sites of the Ar atoms for the $n = 1-4$ clusters. The binding energies of an Ar atom in the vicinity of the Mg^+ ion and attached to an OH group of the water molecule are very similar. The binding of Mg^+ to water leads to a red shift of the OH stretch vibration as a result of the ligand−metal charge transfer similar to that seen previously for other metal cation−water complexes. The binding of the argon atoms leads to additional shifts in the OH stretch vibrational bands. Specifically, attachment of an Ar atom to an OH site leads to a sizable red shift, whereas attachment of Ar atoms to the Mg^+ ion leads to small blue shifts. The spectra are very similar in appearance over the $n = 4-8$ size range, consistent with these larger clusters being dominated by isomers with one Ar atom bound to each OH site, and with the remaining atoms bound in the vicinity of the Mg^+.

This is perhaps the most extensive study to date of weak binding interactions around a metal cation and how these interactions lead to the presence of isomeric structures. The electronic structure calculations correctly identify the main types of isomers present and account in a near quantitative manner for the trend in the vibrational frequencies. However, prediction of the relative energetics of the isomers remains a challenging task, even for the smallest clusters. For the $Mg^+(H_2O)Ar$ and $Mg^+(H_2O)Ar_2$ species, it was shown that it is necessary to adopt large basis sets, e.g., aug-cc-pVQZ, to include electron correlation effects to high order, and to include corrections for vibrational ZPE to correctly identify the more stable isomers. The fact that the spectra calculated for various isomers of the $Mg^+(H_2O)Ar_n$ clusters successfully accounts for the features in the measured spectra indicates that the clusters produced experimentally must be quite cold (T is estimated to be ≤ 50 K).

Rare-gas tagging is essential for the measurement of infrared photodissociation spectroscopy of species such as $Mg^+(H_2O)$ and, as a result, it is important to understand the influence of resulting isomers on the spectroscopy. It would be highly useful to have accurate model potentials for exploring the potential energy landscapes of such clusters. It is hoped that the present study will motivate the development of reliable model potentials for examining Ar-atom binding to metal ion−water systems and to other cation−cluster complexes.

Acknowledgment. We gratefully acknowledge support for this work from National Science Foundation (Duncan grant no. CHE-0244143 and Jordan grant no. CHE-0078528).

References and Notes

(1) Bieske, E. J.; Dopfer, O. *Chem. Rev.* **2000**, *100*, 3963.
(2) Duncan, M. A. *Int. J. Mass Spectrom.* **2000**, *200*, 545.
(3) *Organometallic Ion Chemistry*; Freiser, B. S., Ed.; Kluwer: Dordrecht, The Netherlands, 1996.
(4) *Advances in Metal and Semiconductor Clusters*; Duncan, M. A., Ed.; Elsevier Science: Amsterdam, 2001; Vol. 5.
(5) Marinelli, P. J.; Squires, R. R. *J. Am. Chem. Soc.* **1989**, *111*, 4101.
(6) (a) Dalleska, N. F.; Honma, K.; Sunderlin, L. S.; Armentrout, P. B. *J. Am. Chem. Soc.* **1994**, *116*, 3519. (b) Clemmer, D. E.; Chen, Y.-M.; Aristov, N.; Armentrout, P. B. *J. Phys. Chem.* **1994**, *98*, 7538. (c) Dalleska, N. F.; Tjelta, B. L.; Armentrout, P. B. *J. Phys. Chem.* **1994**, *98*, 4191. (d) Meyer, F.; Khan, F. A.; Armentrout, P. B. *J. Am. Chem. Soc.* **1995**, *117*, 9740. (e) Armentrout, P. B.; Baer, T. *J. Phys. Chem.* **1996**, *100*, 12866. (f) Tjelta, B. L.; Armentrout, P. B. *J. Phys. Chem.* **1997**, *101*, 2064. (g) Sievers, M. R.; Jarvis, L. M.; Armentrout, P. B. *J. Am. Chem. Soc.* **1998**, *120*, 1891. (h) Rogers, M. T.; Armentrout, P. B. *Mass. Spectrom. Rev.* **2000**, *19*, 215. (i) Tjelta, B. L.; Walter, D.; Armentrout, P. B. *Intl. J. Mass. Spectrom.* **2001**, *204*, 7.
(7) Harms, A. C.; Khanna, S. N.; Chen, B.; Castleman, A. W., Jr. *J. Chem. Phys.* **1994**, *100*, 3540.
(8) (a) Beyer, M. B. C.; Gorlitzer, H. W.; Schindler, T.; Achatz, U.; Albert, G.; Niedner-Schatteburg, G.; Bondybey, V. E. *J. Am. Chem. Soc.* **1996**, *118*, 7386. (b) Beyer, M. A.; Achatz, U.; Berg, C.; Joos, S.; Niedner-Schatteburg, G.; Bondybey, V. E. *J. Phys. Chem. A* **1999**, *103*, 671. (c) Bondybey, V. E.; Beyer, M. K. *Int. Rev. Phys. Chem.* **2002**, *21*, 277. (d) Fox, B. S.; Balteanu, I.; Balaj, O. P.; Liu, H.; Beyer, M. K.; Bondybey, V. E. *Phys. Chem. Chem. Phys.* **2002**, *4*, 2224. (e) Berg, C.; Achatz, U.; Beyer, M. K.; Joos, S.; Albert, G.; Schindler, T.; Niedner-Schatteburg, G.; Bondybey, V. E. *Int. J. Mass Spectrom.* **1997**, *167/168*, 723. (f) Berg, C.; Beyer, M. K.; Achatz, U.; Joos, S.; Niedner-Schatteburg, G.; Bondybey, V. E. *Chem. Phys.* **1998**, *239*, 379. (g) Bondybey, V. E.; Beyer, M. K.; Achatz, U.; Fox, B.; Niedner-Schatteburg, G. *Adv. Met., Semicond. Clusters* **2001**, *5*, 295.
(9) Rodriguez-Cruz, S.; Jockusch, R. A.; Williams, E. R. *J. Am. Chem. Soc.* **2002**, *121*, 1986.
(10) (a) Bauschlicher, C. W., Jr.; Partridge, H. *J. Phys. Chem.* **1991**, *95*, 3946. (b) Bauschlicher, C. W., Jr.; Sodupe, M.; Partridge, H. *J. Chem. Phys.* **1992**, *96*, 4453. (c) Partridge, H.; Bauschlicher, C. W., Jr. *Chem. Phys. Lett.* **1992**, *195*, 494.
(11) (a) Watanabe, H.; Iwata, S.; Hashimoto, K.; Misaizu, F.; Fuke, K. *J. Am. Chem. Soc.* **1995**, *117*, 755. (b) Watanabe, H.; Iwata, S. *J. Phys. Chem. A* **1997**, *101*, 487. (c) Watanabe, H.; Iwata, S. *J. Chem.* Phys. **1998**, *108*, 10078. (d) Fuke, K.; Hashimoto, K.; Iwata, S. *Adv. Chem. Phys.* **1999**, *110*, 431. (e) Watanabe, H.; Iwata, S. *J. Phys. Chem.* **1996**, *100*, 3377. (f) Watanabe, H.; Iwata, S. *J. Phys. Chem.* **1996**, *100*, 3377.
(12) (a) Reinhard, B. M.; Niedner-Schatteburg, G. *J. Phys. Chem. A* **2002**, *106*, 7988. (b) Reinhard, B. M.; Niedner-Schatteburg, G. *Phys. Chem. Chem. Phys.* **2002**, *4*, 1471. (c) Reinhard, B. M.; Niedner-Schatteburg, G. *J. Chem. Phys.* **2003**, *118*, 3571.
(13) Markham, G. D.; Glusker, J. P.; Bock, C. W. *J. Phys. Chem. B* **2002**, *106*, 5118.
(14) Lessen, D. E.; Asher, R. L.; Brucat, P. J. *J. Chem. Phys.* **1990**, *93*, 6102.
(15) (a) Willey, K. F.; Yeh, C. S.; Robbins, D.; Pilgrim, J. S.; Duncan, M. A. *J. Chem. Phys.* **1992**, *97*, 8886. (b) Scurlock, C. T.; Pullins, S. H.; Reddic, J. E.; Duncan, M. A. *J. Chem. Phys.* **1996**, *104*, 4591.
(16) (a) Sanekata, M.; Misaizu, F.; Fuke, K. *J. Chem. Phys.* **1996**, *104*, 9768. (b) Misaizu, F.; Sanekata, M.; Tsukamoto, K.; Fuke, K.; Iwata, S. *J. Phys. Chem.* **1992**, *96*, 8259. (c) Sanekata, M.; Misaizu, F.; Fuke, K.; Iwata, S.; Hashimoto, K. *J. Am. Chem. Soc.* **1995**, *117*, 747. (d) Fuke, K.; Hashimoto, K.; Takasu, R. *Adv. Met. Semicond. Clusters* **2001**, *5*, 1. (e) Yoshida, S.; Okai, N.; Fuke, K. *Chem. Phys. Lett.* **2001**, *347*, 93.
(17) (a) Faherty, K. P.; Thompson, C. J.; Aquirre, F.; Michne, J.; Metz, R. B. *J. Phys. Chem.* **2001**, *105*, 10054. (b) Thompson, C. J.; Husband, J.; Aguirre, F.; Metz, R. B. *J. Phys. Chem. A* **2000**, *104*, 8155. (c) Husband, J.; Aguirre, F.; Thompson, C. J.; Laperle, C. M.; Metz, R. B. *J. Phys. Chem. A* **2000**, *104*, 2020.
(18) Wang, K.; Rodham, D. A.; McKoy, V.; Blake, G. A. *J. Chem. Phys.* **1998**, *108*, 4817.
(19) Agreiter, J. K.; Knight, A. M.; Duncan, M. A. *Chem. Phys. Lett.* **1999**, *313*, 162.
(20) (a) Selegue, T. J.; Cabarcos, O. M.; Lisy, J. M. *J. Chem. Phys.* **1994**, *100*, 4790. (b) Cabarcos, O. M.; Weinheimer, C. J.; Lisy, J. M. *J. Chem. Phys.* **1999**, *110*, 8429. (c) Cabarcos, O. M.; Weinheimer, C. J.;

Lisy, J. M. *J. Chem. Phys.* **1998**, *108*, 5151. (d) Lisy, J. M. *Int. Rev. Phys. Chem.* **1997**, *16*, 267. (e) Weinheimer, C. J.; Lisy, J. M. *Int. J. Mass Spectrom. Ion Processes* **1996**, *159*, 197. (f) Weinheimer, C. J.; Lisy, J. M. *J. Phys. Chem.* **1996**, *100*, 15305. (g) Weinheimer, C. J.; Lisy, J. M. *J. Chem. Phys.* **1996**, *105*, 2938. (h) Lisy, J. M. *Cluster Ions* **1993**, 217, Editors: C. Ng, T. Baer, I. Powis, Wiley: Chichester, U.K. (i) Vaden, T. D.; Forinash, B.; Lisy, J. M. *J. Chem. Phys.* **2002**, *117*, 4628. (j) Vaden, T. D.; Weinheimer, C. J.; Lisy, J. M. *J. Chem. Phys.* **2004**, *121*, 3102.

(21) (a) Walker, N. R.; Walters, R. S.; Pillai, E. D.; Duncan, M. A. *J. Chem. Phys.* **2003**, *119*, 10471. (b) Walters, R. S.; Duncan, M. A. *Aust. J. Chem.* **2004**, *57*, 1145. (c) Walters, R. S.; Duncan, M. A. To be published.

(22) (a) Inokuchi, Y.; Ohshimo, K.; Misaizu, F.; Nishi, N. *Chem. Phys. Lett.* **2004**, *390*, 140. (b) Inokuchi, Y.; Ohshimo, K.; Misaizu, F.; Nishi, N. *J. Phys. Chem. A* **2004**, *108*, 5034.

(23) (a) Yeh, C. S.; Pilgrim, J. S.; Robbins, D. L.; Willey, K. F.; Duncan, M. A. *Int. Rev. Phys. Chem.* **1994**, *13*, 231. (b) Pilgrim, J. S.; Berry, K. R.; Duncan, M. A. *J. Chem. Phys.* **1994**, *100*, 7945. (c) Willey, K. F.; Yeh, C. S.; Robbins, D. L.; Duncan, M. A. *J. Chem. Phys.* **1993**, *98*, 1867. (d) Reddic, J. E.; Duncan, M. A. *J. Chem. Phys.* **1999**, *110*, 9948. (e) Pullins, S. H.; Scurlock, C. T.; Reddic, J. E.; Duncan, M. A. *J. Chem. Phys.* **1996**, *104*, 7518. (f) France, M. R.; Pullins, S. H.; Duncan, M. A. *J. Chem. Phys.* **1998**, *109*, 8842. (g) Duncan, M. A. *Annu. Rev. Phys. Chem.* **1997**, *48*, 69.

(24) (a) Gregoire, G.; Duncan, M. A. *J. Chem. Phys.* **2002**, *117*, 2120. (b) Gregoire, G.; Brinkmann, N. R.; van Heijnsbergen, D.; Schaefer, H. F.; Duncan, M. A. *J. Phys. Chem. A* **2003**, *107*, 218. (c) Walters, R. S.; Jaeger, T. D.; Brinkman, N. R.; Schaefer, H. F.; Duncan, M. A. *J. Phys. Chem. A* **2003**, *107*, 7396. (d) Jaeger, J. B.; Jaeger, T. D.; Brinkmann, N. R.; Schaefer, H. F.; Duncan, M. A. *Can. J.* Chem. **2004**, *82*, 934. (e) Walker, N. R.; Walters, R. S.; Duncan, M. A. *J. Chem. Phys.* **2004**, *120*, 10037. (f) Walker, N. R.; Grieves, G. A.; Walters, R. S.; Duncan, M. A. *J. Chem. Phys.* **2004**, *121*, 10498.

(25) Duncan, M. A. *Intl. Rev. Phys. Chem.* **2003**, *22*, 407.

(26) (a) Okumura, M.; Yeh, L. I.; Lee, Y. T. *J. Chem. Phys.* **1985**, *83*, 3705. (b) Okumura, M.; Yeh, L. I.; Lee, Y. T. *J. Chem. Phys.* **1988**, *88*, 79. (c) Yeh, L. I.; Okumura, M.; Myers, J. D.; Price, J. M.; Lee, Y. T. *J. Chem. Phys.* **1989**, *91*, 7319.

(27) Linnartz, H.; Verdes, D.; Maier, J. P. *Science* **2002**, *297*, 1166.

(28) (a) Fuji, A.; Fujimaki, E.; Ebata, T.; Mikami, N. *J. Chem. Phys.* **2000**, *112*, 6275. (b) Fujimaki, E.; Fuji, A.; Ebata, T.; Mikami, N. *J. Phys. Chem.* **2001**, *105*, 4882.

(29) Pino, T.; Boudin, N.; Brechignac, P. *J. Chem. Phys.* **1999**, *111*, 7337.

(30) (a) Nizkorodov, S. A.; Dopfer, O.; Ruchti, T.; Meuwly, M.; Maier, J. P.; Bieske, E. J. *J. Phys. Chem.* **1995**, *99*, 17118. (b) Dopfer, O.; Nizkorodov, S. A.; Meuwly, M.; Bieske, E. J.; Maier, J. P. *Intl. J. Mass Spectrom., Ion Processes* **1997**, *167/168*, 637. (c) Olkhov, R. V.; Nizkorodov, S. A.; Dopfer, O. *Chem. Phys.* **1998**, *239*, 393. (d) Olkhov, R. V.; Nizkorodov, S. A.; Dopfer, O. *J. Chem. Phys.* **1998**, *108*, 1. (e) Dopfer, O.; Roth, D.; Maier, J. P. *J. Phys. Chem. A* **2000**, *104*, 11702. (f) Dopfer, O.; Roth, D.; Maier, J. P. *J. Chem. Phys.* **2001**, *114*, 7081.

(31) (a) Bailey, C. G.; Kim, J.; Dessent, C. E. H.; Johnson, M. A. *Chem. Phys. Lett.* **1997**, *269*, 122. (b) Ayotte, P.; Weddle, G. H.; Kim, J.; Johnson, M. A. *Chem. Phys.* **1998**, *239*, 485. (c) Ayotte, P.; Weddle, G. H.; Kim, J.; Johnson, M. A. *J. Am. Chem. Soc.* **1998**, *120*, 12361. (d) Ayotte, P.; Bailey, C. G.; Kim, J.; Johnson, M. A. *J. Chem. Phys.* **1998**, *108*, 444. (e) Nielson, S. B.; Ayotte, P.; Kelley, J. A.; Johnson, M. A. *J. Chem. Phys.* **1999**, *111*, 9593. (f) Price, E. A.; Robertson, W. H.; Diken, E. G.; Weddle, G. H.; Johnson, M. A. *Chem. Phys. Lett.* **2002**, *366*, 412. (g) Corcelli, S. A.; Kelley, J. A.; Tully, J. C.; Johnson, M. A. *J. Phys. Chem. A* **2002**, *106*, 4872. (h) Robertson, W. H.; Johnson, M. A. *Annu. Rev. Phys. Chem.* **2003**, *54*, 173. (i) Hammer, N. I.; Shin, J.-W.; Headrick, J. M.; Diken, E. G.; Roscoli, J. R.; Weddle, G. H.; Johnson, M. A. *Science* **2004**, *306*, 675. (j) Diken, E. G.; Headrick, J. M.; Roscoli, J. R.; Bopp, J. C.; Johnson, M. A. *J. Phys. Chem. A* **2005**, *109*, 1487.

(32) Nakanaga, T.; Ito, F. *Chem. Phys. Lett.* **2002**, *355*, 109.

(33) (a) Jaeger, T. D.; Duncan, M. A. *J. Phys. Chem. A* **2004**, *108*, 6605. (b) Jaeger, T. D.; Duncan, M. A. *J. Phys. Chem. A* **2005**, *109*, 3311. (c) Walters, R. S.; Jaeger, T. D.; Duncan, M. A. *J. Phys. Chem. A* **2002**, *106*, 10482. (d) Walters, R. S.; Schleyer, P. v. R, Corminboeuf, C.; Duncan, M. A. *J. Am. Chem. Soc.* **2005**, *127*, 1100.

(34) Frisch, M. J.; Trucks, G. W.; Schlegel, H. B.; Scuseria, G. E.; Robb, M. A.; Cheeseman, J. R.; Montgomery, J. A.; Vreven, T.; Kudin, K. N.; Burant, J. C.; Millam, J. M.; Iyengar, S. S.; Tomasi, J.; Barone, V.; Mennucci, B.; Cossi, M.; Scalmani, G.; Rega, N.; Petersson, G. A.; Nakatsuji, H.; Hada, M.; Ehara, M.; Toyota, K.; Fukuda, R.; Hasegawa, J.; Ishida, M.; Nakajima, T.; Honda, Y.; Kitao, O.; Nakai, H.; Klene, M.; Li, X.; Knox, J. E.; Hratchian, H. P.; Cross, J. B.; Adamo, C.; Jaramillo, J.; Gomperts, R.; Stratmann, R. E.; Yazyev, O.; Austin, A. J.; Cammi, R.; Pomelli, C.; Ochterski, J. W.; Ayala, P. Y.; Morokuma, K.; Voth, G. A.; Salvador, P.; Dannenberg, J. J.; Zakrzewski, V. G.; Dapprich, S.; Daniels, A. D.; Strain, M. C.; Farkas, O.; Malick, D. K.; Rabuck, A. D.; Raghavachari, K.; Foresman, J. B.; Ortiz, J. V.; Cui, Q.; Baboul, A. G.; Clifford, S.; Cioslowski, J.; Stefanov, B. B.; Liu, G.; Liashenko, A.; Piskorz, P.; Komaromi, I.; Martin, R. L.; Fox, D. J.; Keith, T.; Al-Laham, M. A.; Peng, C. Y.; Nanayakkara, A.; Challacombe, M.; Gill, P. M. W.; Johnson, B.; Chen, W.; Wong, M. W.; Gonzalez, C.; Pople, J. A. *Gaussian 03*, Revision A.1; Gaussian, Inc.: Pittsburgh, PA, 2003.

(35) (a) Dunning, T. H., Jr. *J. Chem. Phys.* **1989**, *90*, 1007. (b) Kendall, R. A.; Dunning, T. H., Jr.; Harrison, R. J. *J. Chem. Phys.* **1992**, *96*, 6796. (c) Woon, D. E.; Dunning, T. H., Jr. *J. Chem. Phys.* **1993**, *98*, 1358.

(36) Pople, J. A.; Head-Gordan, M.; Raghavachari, K. *J. Chem. Phys.* **1987**, *87*, 5968.

(37) Fuentealba, P.; Szentpaly, L. V.; Preuss, H.; Stoll, H. *J. Phys. B* **1985**, *18*, 1287.

(38) Nicklass, A.; Dolg, M.; Stoll, H.; Preuss, H. *J. Chem. Phys.* **1995**, *102*, 8942.

(39) Boys, S. F.; Bernardi, F. *Mol. Phys.* **1970**, *19*, 553.

(40) Simon, S.; Duran, M.; Dannenberg, J. J. *J. Chem. Phys.* **1996**, *105*, 11024.

(41) Shimanouchi, T. *Molecular Vibrational Frequencies*, 69th ed.; Chemistry WebBook, NIST Standard Reference Database (http://webbook.nist.gov), 2001.